



OPEN

# TMEM101 expression and its impact on immune cell infiltration and prognosis in hepatocellular carcinoma

Lingyun Kuang<sup>1</sup>, Yilin Pang<sup>2</sup> & Quangang Fang<sup>1</sup>✉

Hepatocellular carcinoma (HCC) is a cancer caused by inflammation, which affects the immune response and treatment outcomes. Finding new immune-related targets could improve HCC immunotherapy. New research suggests that TMEM family proteins can act as either tumor suppressors or oncogenes, but the role of TMEM101 in HCC development is unclear. This study conducted an analysis of TMEM101 mRNA expression and its correlation with clinical outcomes in HCC patients using RNA sequencing data from various open databases. Additionally, differences in TMEM101 expression in HCC cell lines and HCC tissue microarrays were examined using RT-qPCR, western blotting, and *in situ* hybridization staining. The findings presented herein offer initial evidence indicating a significant upregulation of TMEM101 mRNA expression in HCC, which is linked to a poorer prognosis. Furthermore, TMEM101 expression was found to be positively associated with the histological grade and clinical stage of HCC patients. Moreover, a notable reduction in promoter methylation of TMEM101 was observed in HCC patients. Cox regression analysis indicated that TMEM101 was an independent prognostic factor for overall survival (OS) in HCC patients. A nomogram incorporating TMEM101 and tumor stage was constructed and assessed. Comparative analysis with four established HCC diagnostic biomarkers (AFP, EFNA3, MDK, and SMYD5) using ROC curve and time-dependent ROC curves demonstrated the diagnostic potential of TMEM101 in HCC. Gene set enrichment analysis (GSEA) revealed a correlation between TMEM101 and the cell cycle, DNA replication, and repair signaling pathways, which were differentially enriched in the TMEM101 high expression phenotype. The findings from CIBERSORT analysis suggest that TMEM101's pro-tumor effect may be due to decreasing the number of anti-tumor immune cells (M1 macrophages and resting memory CD4<sup>+</sup> T cells) and promoting M0 macrophage infiltration in the tumor microenvironment (TME). Overall, our study indicates that TMEM101 could serve as a promising diagnostic and prognostic biomarker for HCC.

**Keywords** TMEM101, Hepatocellular carcinoma, Prognostic biomarker, Immune infiltrates, Immunotherapy

Hepatocellular carcinoma (HCC) is a form of primary liver cancer characterized by a high mortality rate<sup>1</sup>. The absence of discernible symptoms in the initial stages of HCC frequently results in diagnostic delays. While curative interventions such as hepatectomy, thermal ablation, chemotherapy, and interventional therapies are commonly employed for early-stage cases, the efficacy of these treatments is often hindered by high rates of relapse or metastasis in HCC patients<sup>2,3</sup>. Consequently, there is an urgent need for more extensive research into the pathogenesis of HCC and the discovery of novel biomarkers to accurately predict the prognosis of individuals with HCC. Furthermore, ongoing exploration of new biomarkers can enhance the diagnostic effectiveness of clinical biomarkers for HCC. For instance, Christou *et al.*<sup>4</sup> demonstrated that midkine (MDK) serves as a robust biomarker for early detection of HCC, particularly in individuals who test negative for  $\alpha$ -fetoprotein (AFP). While MDK may exhibit lower specificity compared to AFP, it demonstrates markedly higher sensitivity<sup>4</sup>.

<sup>1</sup>Jiangxi Provincial People's Hospital, The First Affiliated Hospital of Nanchang Medical College, 152 Aiguo Road, Nanchang 330006, Jiangxi, China. <sup>2</sup>Zhejiang Provincial Key Laboratory of Medical Genetics, Key Laboratory of Laboratory Medicine, School of Laboratory Medicine and Life Sciences, Ministry of Education, Wenzhou Medical University, Wenzhou 325035, Zhejiang, China. ✉email: 173224668@qq.com

Previous studies have indicated that the tumor microenvironment (TME) plays a critical role in the development and progression of HCC<sup>5</sup>. The TME consists of aberrant extracellular matrix (ECM), immune cells, cancer-associated fibroblasts (CAFs), tumor-associated endothelial cells (TECs), or macrophages (TAMs) and their cellular products<sup>6</sup>. The application of immune checkpoint inhibitors (ICIs) has significantly improved the therapeutic outcomes for HCC patients, leading to extended survival in those who exhibit a positive response to ICIs<sup>7</sup>. For example, the co-administration of atezolizumab and bevacizumab has demonstrated superior OS compared to sorafenib, resulting in the approval of this combination therapy by the Food and Drug Administration (FDA)<sup>8</sup>. Nevertheless, despite the significant progress made in immunotherapy for HCC through ICIs, the intricate pathogenesis of HCC and the immunosuppressive TME contribute to response rates of less than 20% for ICIs monotherapy and approximately 30–36% for combination therapy<sup>7</sup>. This underscores the critical necessity for identifying novel immune-related therapy targets for patients with HCC.

Transmembrane proteins (TMEM) are a class of integral membrane proteins that traverse biological membranes and are permanently embedded within them<sup>9,10</sup>. In recent years, many studies have revealed differential expression of TMEM in tumor tissues compared to neighboring healthy tissues, with some TMEM proteins acting as tumor suppressors or oncogenes<sup>10</sup>. Matsuda *et al.*<sup>11</sup> have suggested that TMEM101 may play a role in activating NF- $\kappa$ B signaling pathways, although the precise molecular function of TMEM101 is still not fully understood. In this study, our results demonstrated that TMEM101 associated with immune infiltration serves as a prognostic biomarker in HCC. Thus, the findings of this study may help us to understand the role of TMEM101 in the occurrence and development of HCC.

## Results

### Clinical characteristics of patients

The study cohort consisted of 377 primary tumors with clinical and gene expression data obtained from TCGA, encompassing variables such as age, histological grade, clinical stage, TNM stage, and sex. Among the tumors, 14.78% were well differentiated, 48.39% were moderately differentiated, and 36.82% were poorly differentiated. Regarding HCC stage, 175 patients were classified as stage I (49.58%), 87 as stage II (24.65%), 86 as stage III (24.36%), and 5 as stage IV (1.42%), as indicated in Table 1.

### High TMEM101 expression in HCC

In comparison to normal liver tissues, TMEM101 exhibits higher expression levels in HCC, as demonstrated through boxplots and paired differential plots (Fig. 1A,B). These findings were further validated in the

Clinical characteristics	Total (377)	%
Age		
≤ 60	180	47.87
> 61	196	52.13
Histological grade		
G1	55	14.78
G2	180	48.39
G3	124	33.33
G4	13	3.49
Clinical stage		
Stage I	175	49.58
Stage II	87	24.65
Stage III	86	24.36
Stage IV	5	1.42
Sex		
Female	122	32.36
Male	255	67.64
T stage		
T1	185	49.47
T2	95	25.40
T3	81	21.66
T4	13	38.24
N stage		
N0	257	98.47
N1	4	1.53
M stage		
M0	272	98.55
M1	4	1.45

**Table 1.** Clinical characteristics of HCC patients were obtained from the TCGA database.

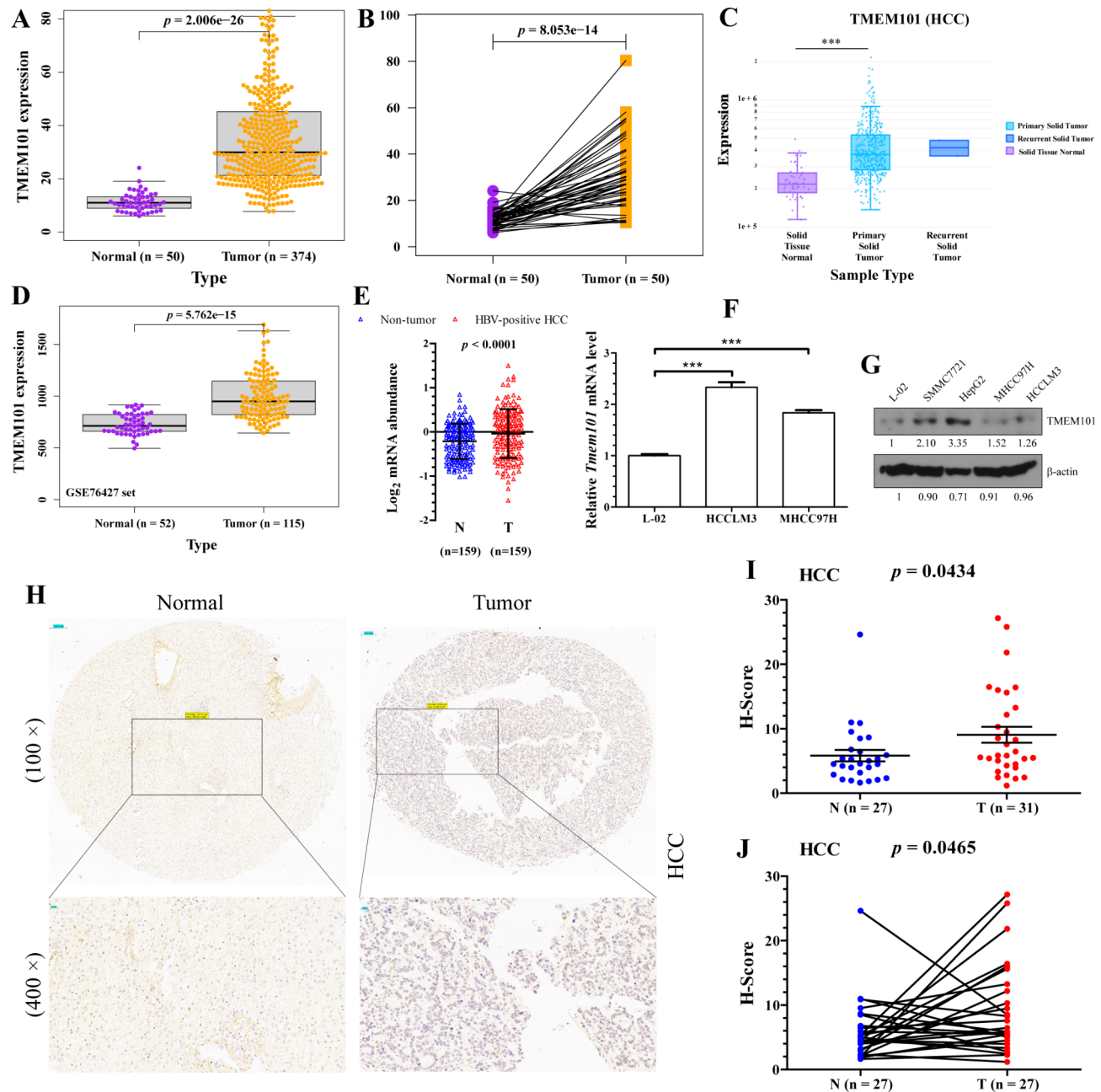


**Fig. 1.** TMEM101 transcription expression in HCC and adjacent normal liver tissues. (A) The expression of TMEM101 within HCC tissues and adjacent normal liver tissues was examined using RNA-seq (TCGA). (B) Paired expression data of TMEM101 mRNA in HCC and adjacent normal tissues by RNA-Seq in TCGA dataset. (C) mRNA expression of TMEM101 in primary solid tumor, recurrent solid tumor, and adjacent normal liver tissues (DriverDBV3 database). (D) Box plot showing TMEM101 mRNA expression levels in GSE76427 set. (E) The expression levels of TMEM101 mRNA in HBV-associated HCC and matched non-tumor liver tissues were quantified with RNA-seq ( $n=159$ ). These findings were acquired from the research of Gao *et al.*<sup>[12]</sup>. (F) Real-time qPCR analysis of TMEM101 mRNA expression in human hepatocytes and HCC cell lines. (G) The expression levels of TMEM101 protein in various liver cancer cell lines were analyzed via Western Blot in comparison to the normal liver cell line L-02. (H) Representative in situ hybridization images (DAB staining) of TMEM101 in HCC and adjacent normal tissues. (I) H-score summary statistics were calculated for HCC and non-tumor liver tissues. (J) Relative expression levels of TMEM101 in HCC and corresponding normal tissues.  $***, p < 0.001$ .

DriverDBV3 database and GSE76427 dataset (Fig. 1C-D). Moreover, TMEM101 mRNA levels were significantly elevated in HCC patients with hepatitis B virus (HBV) infection (Fig. 1E<sup>[12]</sup>). Consistently, elevated TMEM101 mRNA levels were observed in HCC cell lines compared to normal human L-02 hepatocytes (Fig. 1F and Supplementary Table S3). Further, western blot analysis revealed that TMEM101 protein levels were significantly

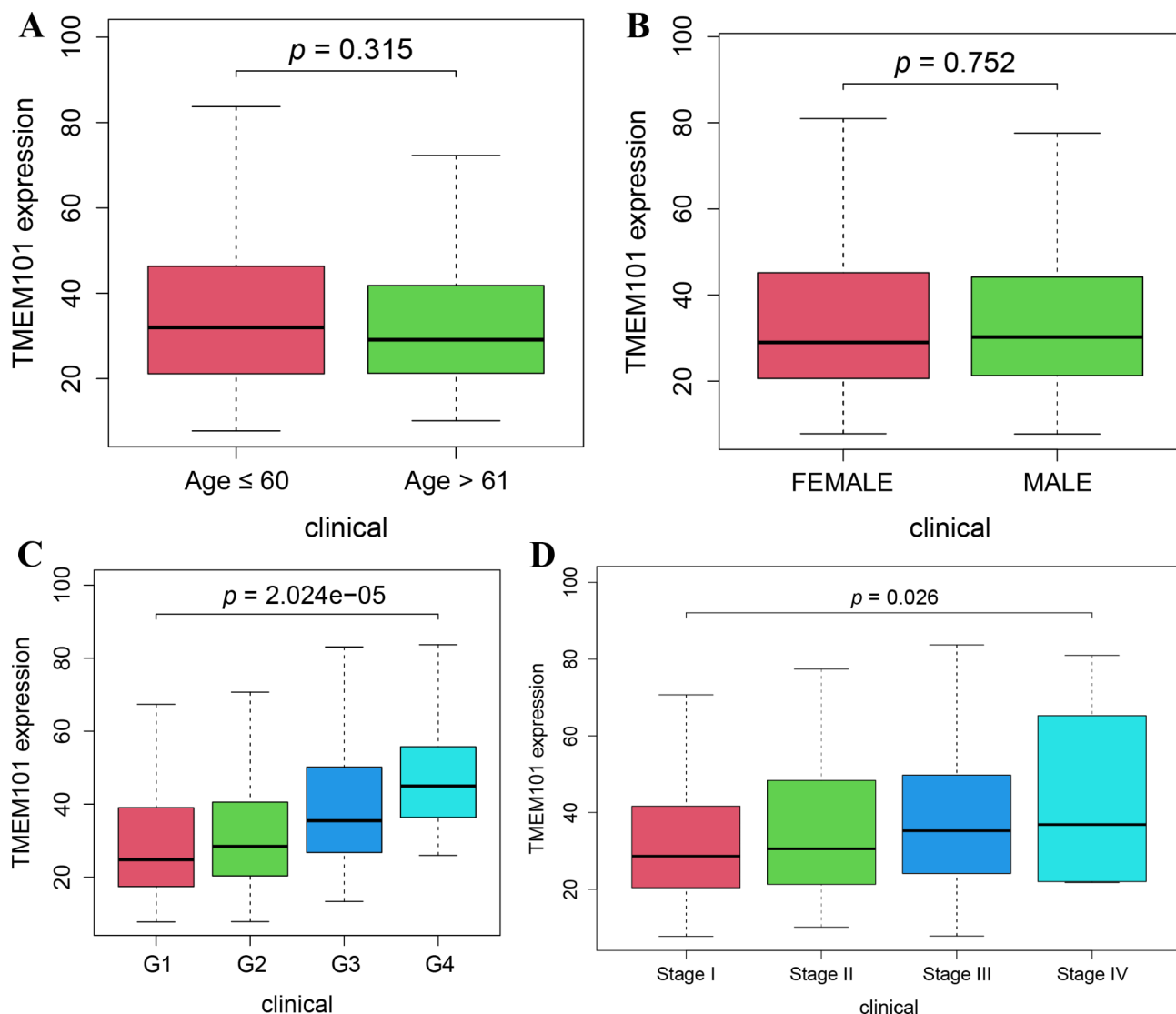
higher in the SMMC7721, HepG2, MHCC97H, and HCCLM3 liver cancer cell lines compared to the L-02 cells (Fig. 1G and Supplementary Fig. S1). To confirm TCGA database findings, *in situ* hybridization was used to examine TMEM101 mRNA expression (Supplementary Fig. S2). Using the Aipathwell Image Analysis system, the data showed that TMEM101 mRNA was significantly more expressed in liver cancer tissues than in adjacent normal tissues (Fig. 1H-I). Analysis of matched samples ( $n=27$ ) confirmed that HCC tissues had significantly elevated TMEM101 mRNA levels (Fig. 1J,  $p < 0.05$ ).

#### The relationship between TMEM101 and the clinical characteristics of HCC patients

The findings presented in Fig. 2 indicate a positive correlation between elevated levels of TMEM101 mRNA and both histological grade ( $p < 0.001$ ) and clinical stage ( $p < 0.05$ ). Logistic regression analysis was employed to investigate the association between TMEM101 expression and clinical features in patients with HCC. The results revealed a significant correlation between increased TMEM101 mRNA levels and higher grade (Grade 3 vs. Grade 1,  $p < 0.05$ ; Grade 4 vs. Grade 1,  $p < 0.05$ ) and pathological stage (Stage III vs. Stage I,  $p < 0.01$ ) in HCC (Table 2). These results imply that HCC patients exhibiting heightened TMEM101 expression are more prone to advanced stages of the disease compared to those with lower TMEM101 expression levels.

#### Decreased TMEM101 promoter methylation levels in HCC

To investigate the disparity in mRNA expression levels of TMEM101 between HCC cases and normal controls, the UALCAN database was utilized to assess the association between TMEM101 expression and its promoter DNA methylation. Figure 3A illustrates that the promoter methylation levels of TMEM101 were diminished in HCC tissues compared to adjacent normal liver tissues. Subsequently, an examination of TMEM101 promoter DNA methylation across various subgroups based on distinct clinicopathological parameters was conducted to

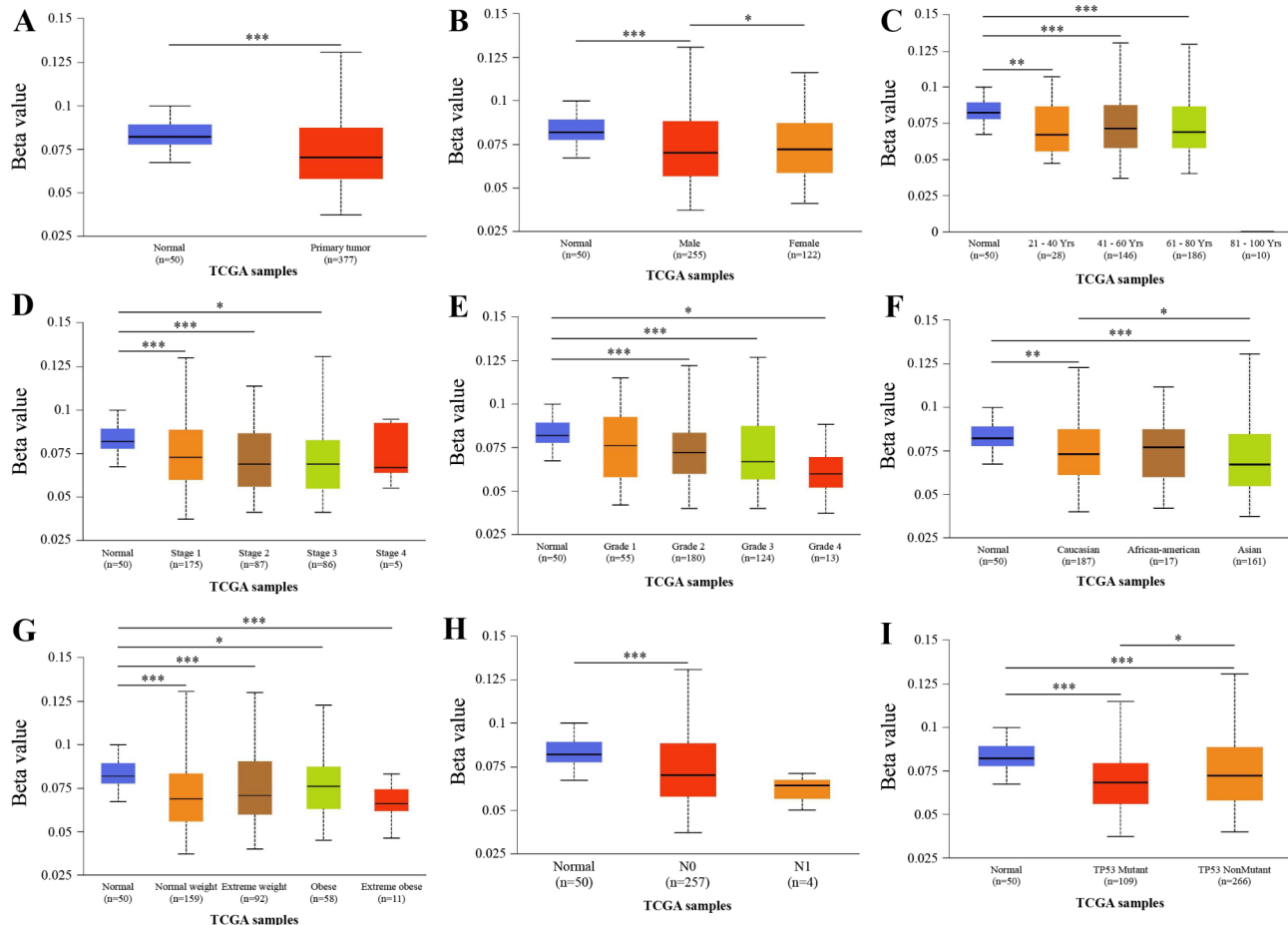


**Fig. 2.** The relationship between TMEM101 expression and clinical characteristics. (A) Age; (B) Gender; (C) Tumor grade; (D) Clinical stage.

Clinical characteristics	Total (N)	Odds ratio in TMEM101 expression	p-Value
Age			
>61 vs. ≤ 60	370	0.7542 (0.5004–1.1346)	0.1764
Gender			
Male vs. Female	371	1.1780 (0.7630–1.8221)	0.4600
Tumor differentiation			
Grade 2 vs. Grade 1	232	0.9719 (0.5289–1.8010)	0.9272
Grade 3 vs. Grade 1	177	1.9243 (1.0140–3.6924)	<b>0.0464</b>
Grade 4 vs. Grade 1	67	6.4583 (1.5238–44.6534)	<b>0.0231</b>
Pathological stage			
Stage II vs. Stage I	257	1.3108 (0.7792–2.2080)	0.3075
Stage III vs. Stage I	256	2.1710 (1.2804–3.7262)	<b>0.0044</b>
Stage IV vs. Stage I	176	1.9662 (0.3181–15.2127)	0.4652

**Table 2.** *TMEM101* expression<sup>a</sup> is associated with clinical pathological characteristics (logistic regression).

<sup>a</sup>Categorical dependent variable, greater or less than the median expression level. A bold *p*-value signifies statistical significance.

**Fig. 3.** Promoter methylation level of TMEM101 in HCC (UALCAN). (A) Promoter methylation level of TMEM101 in normal and HCC patients. (B–I) TMEM101 promoter methylation levels of HCC patients in subgroups with different genders, ages, individual cancer stages, tumor grades, races, weights, nodal metastasis status, and TP53 mutation status. Data are shown as mean ± SE. \*, *p* < 0.05; \*\*, *p* < 0.01; \*\*\*, *p* < 0.001.

elucidate the factors influencing TMEM101 promoter methylation levels. The subgroup analysis results indicated that the methylation of the TMEM101 promoter in HCC may be influenced by various factors including gender, age, cancer stage, tumor grade, race, weight, nodal metastasis status, and TP53 mutation status (Fig. 3B–I). Specifically, higher levels of TMEM101 promoter methylation were associated with more advanced and less

differentiated tumors in HCC patients, who exhibited lower levels of promoter methylation (Fig. 3D-E) and higher TMEM101 mRNA expression levels (Fig. 2C-D).

### Frequency and types of TMEM101 alterations in HCC

Subsequently, an analysis was conducted on genetic alterations in TMEM101 and their correlation with OS and DFS among patients with HCC. Among the 360 HCC patients who were sequenced, 43 exhibited genetic alterations, resulting in a mutation rate of 12% (Fig. 4A). Notably, mRNA upregulation emerged as the predominant form of genetic alteration involving TMEM101 in HCC (Fig. 4A). Furthermore, findings from the Kaplan-Meier plot and log-rank test demonstrated a significant association between genetic alterations in TMEM101 and reduced DFS (Fig. 4B,  $p=6.292\text{e-}3$ ) and OS (Fig. 4C,  $p=5.150\text{e-}3$ ) in HCC patients. These findings suggest that genetic alterations in TMEM101 may have a substantial impact on the prognosis of HCC patients.

### Survival analysis and clinical diagnostic efficacy of TMEM101

Kaplan-Meier survival analysis was utilized to assess the prognostic significance of TMEM101 expression in patients with HCC. The findings indicated a correlation between high TMEM101 expression levels and unfavorable prognosis ( $p=0.005$ ) (Fig. 4D). To further confirm the predictive capability of TMEM101, a Kaplan-Meier curve was generated using data from the International Cancer Genome Consortium (ICGC) dataset. Consistent with results from TCGA cohort, patients with high TMEM101 expression exhibited significantly lower OS rates compared to those with low TMEM101 expression ( $p=0.003$ ) (Fig. 4E). Additionally, receiver operating characteristic (ROC) curve analysis was performed on TMEM101 gene expression data to assess its diagnostic utility. The resulting area under the ROC curve (AUC) was calculated to be 0.963, suggesting a high diagnostic value for TMEM101 (Fig. 4F).

### High expression of TMEM101 may be an independent predictor of prognosis in HCC

Further, we conducted an evaluation of prognostic factors associated with OS through univariate and multivariate Cox regression analyses (Fig. 5). The results of the univariate Cox model analysis revealed a significant correlation

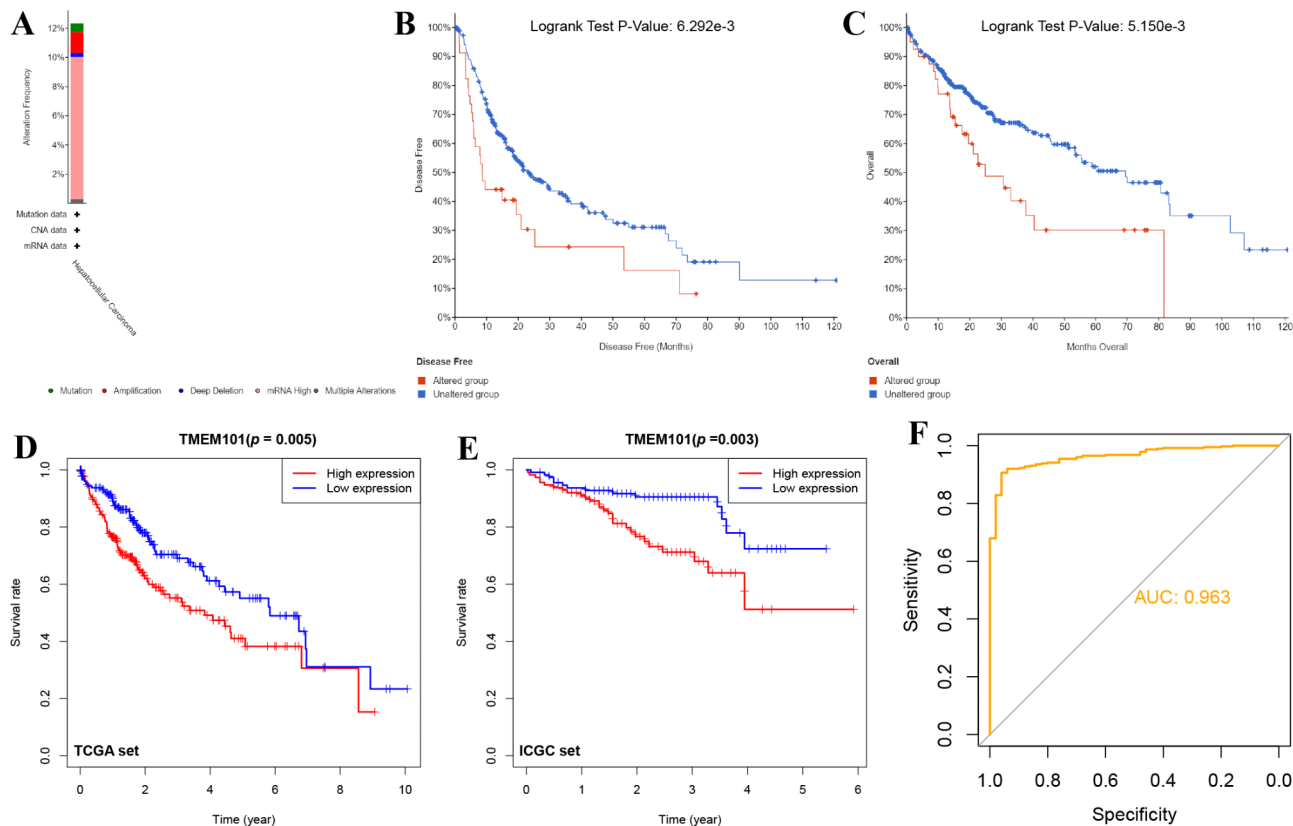


**Fig. 4.** Genetic alterations, prognostic and diagnostic value of TMEM101 in HCC patients. (A) OncoPrint in cBioPortal showed the alteration frequency of TMEM101 in HCC. The different types of genetic alterations are highlighted in different colors. (B-C) Genetic alterations in TMEM101 were associated with shorter DFS (B) and OS (C) of HCC patients (cBioPortal database). (D) High expression of TMEM101 was correlated with worse OS in HCC patients. (E) Kaplan-Meier survival analysis of the prognostic value of TMEM101 in the ICGC validation set. (F) The ROC curve demonstrated the diagnostic value of TMEM101 in HCC patients. Abbreviations: OS: overall survival; DFS: disease free survival.

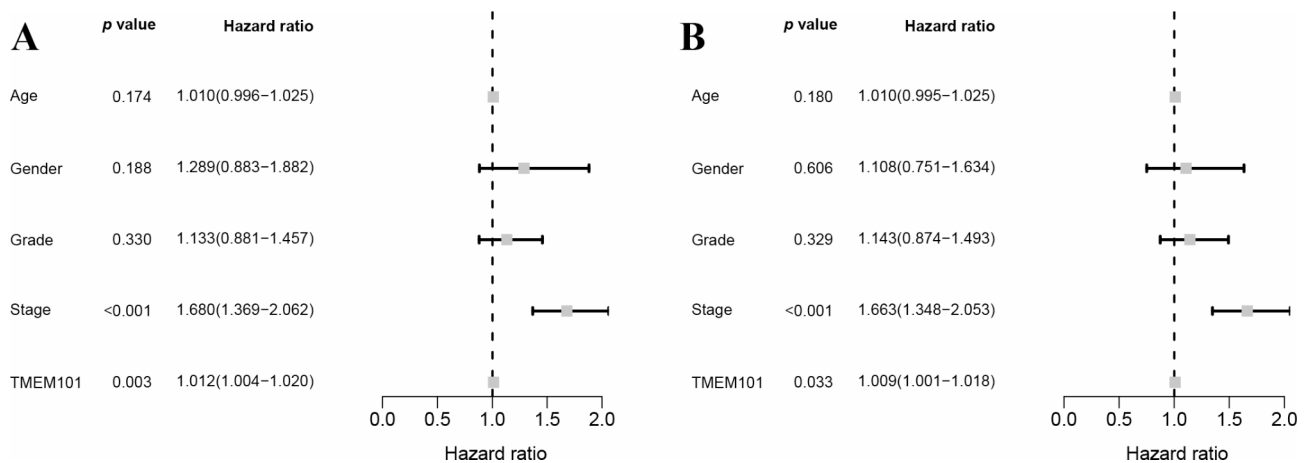


**Fig. 5.** Forest plots show univariate (A) and multivariate (B) Cox regression analysis of the relationship between TMEM101 expression and HCC patient survival.

between high TMEM101 expression and decreased OS (hazard ratio [HR] = 1.012, 95%CI = 1.004–1.020,  $p = 0.003$ ). Additionally, other clinicopathologic variables, such as pathological stage, were found to be linked to poor survival outcomes (Fig. 5A). Subsequent multivariate Cox analysis further supported TMEM101 gene expression (HR = 1.009, 95%CI = 1.001–1.018,  $p = 0.033$ ) and pathological stage (HR = 1.663, 95%CI = 1.348–2.053,  $p < 0.001$ ) as independent risk factors for OS in patients with HCC, as depicted in Fig. 5B.

### Building a predictive nomogram

To facilitate the clinical utilization of elevated TMEM101 expression, a comprehensive nomogram was devised by amalgamating two distinct prognostic indicators, namely TMEM101 expression level and tumor stage. This nomogram enabled clinicians to forecast patient prognosis based on cumulative points. Patients with higher total points exhibited inferior survival outcomes, as depicted in Fig. 6A. Calibration curves (Fig. 6B–D) demonstrated a favorable concordance between the nomogram-projected OS and the observed OS, underscoring the practical value of this integrated nomogram.

### In contrast to other established biomarkers, TMEM101 demonstrates superior predictive capability for OS in patients with HCC

In Fig. 7, we conducted a comparative analysis to validate the predictive efficacy of four HCC diagnostic biomarkers (AFP<sup>13</sup>, EFNA3<sup>14</sup>, MDK<sup>4</sup>, and SMYD5<sup>15</sup>) documented in existing literature. The boxplots illustrate that AFP, EFNA3, MDK, and SMYD5 exhibit higher expression levels in HCC samples compared to normal liver tissues (Fig. 7A–D). Furthermore, the ROC curve analysis demonstrated that the AUC values for AFP, EFNA3, MDK, and SMYD5 were 0.723, 0.927, 0.948, and 0.937, respectively (Fig. 7E–H). The results of time-dependent ROC analysis indicate that the AUC values for predicting 1-year, 3-year, and 5-year OS of TMEM101 and EFNA3 were 0.661, 0.615, 0.603, and 0.676, 0.664, 0.616, respectively (Fig. 7I–K). In contrast, the AUC values for AFP, MDK, and SMYD5 were 0.636, 0.624, and 0.712 at 1 year, 0.545, 0.613, and 0.623 at 3 years, and 0.526, 0.570, and 0.593 at 5 years. In summary, TMEM101 and EFNA3 (AUC > 0.6) demonstrated superior performance in predicting OS of HCC patients compared to AFP, MDK, and SMYD5.

### Signaling pathways associated with TMEM101 expression

To explore the signaling pathways and biological functions associated with TMEM101 in HCC, we conducted an enrichment analysis using GSEA. Significantly enriched pathways were identified based on criteria including a  $p$ -value  $< 0.05$ , false discovery rate (FDR)  $< 0.05$ , and normalized enrichment score (NES). The findings suggest a correlation between high TMEM101 expression phenotype and various signaling pathways, including base excision repair, mismatch repair, nucleotide excision repair, DNA replication, cell cycle, pathways in cancer, and notch signaling pathway (Fig. 8A; Table 3). Conversely, the significantly enriched signaling pathways in the low TMEM101 expression phenotype encompass alanine, aspartate and glutamate metabolism, arginine and proline metabolism, citrate cycle TCA cycle, fatty acid metabolism, glycine, serine and threonine metabolism, linoleic acid metabolism, PPAR signaling pathway, retinol metabolism, tryptophan metabolism, and valine, leucine and isoleucine degradation (Fig. 8B; Table 4).

### The association between TMEM101 expression and the proportion of tumor-infiltrating immune cells

Additionally, to validate the association between TMEM101 expression and the immune microenvironment, the distribution of tumor-infiltrating immune subsets was examined utilizing the CIBERSORT algorithm, with an evaluation of 22 distinct immune cell profiles in patients with HCC (Fig. 9A). Furthermore, the correlation matrix analysis indicated that activated memory CD4<sup>+</sup> T cells exhibited the most robust positive correlation with CD8<sup>+</sup> T cells, while neutrophils were positively associated with activated mast cells. Conversely, M0 macrophages

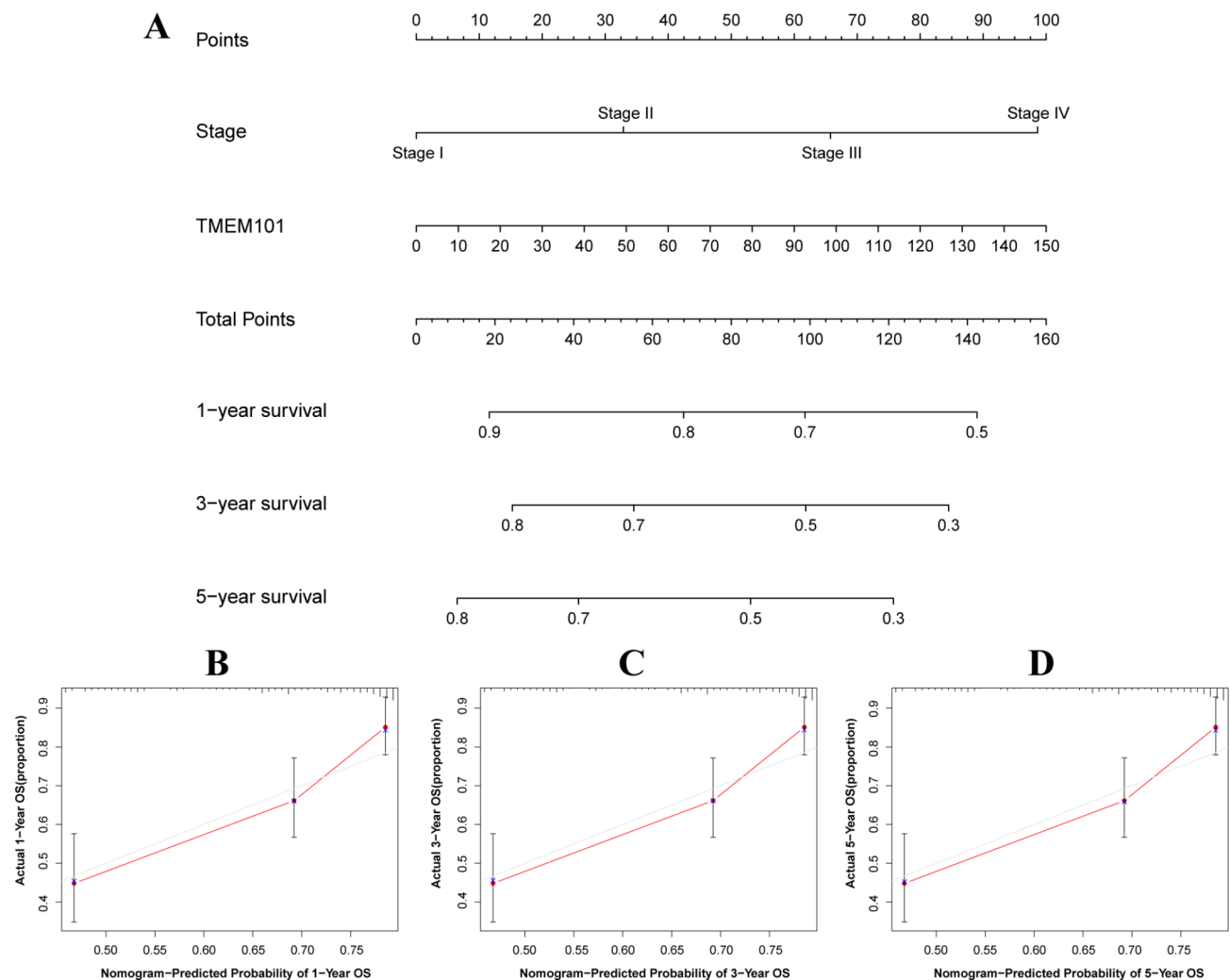


**Fig. 6.** Nomogram for predicting probability of patients with 1-, 3-, and 5-year OS. For risk estimation, identify the status for each clinical factor and expression value of TMEM101, draw a line straight upwards to the Points axis to see the points a single factor yields. Repeat until scores for all factors are decided. Sum the points and locate the summed point on the Total Points axis. Then 1-, 3-, and 5-years-related survival probabilities were obtained by drawing a line straight down to the Risk axis.

demonstrated a negative correlation with CD8<sup>+</sup> T cells and naive B cells (Fig. 9B). Based on the median expression level of TMEM101, the samples were stratified into high and low subgroups, revealing statistically significant variances among three cell types: resting memory CD4<sup>+</sup> T cells ( $p=0.039$ ), M0 macrophages ( $p=0.038$ ), and M1 macrophages ( $p=0.031$ ) (Fig. 9C).

#### The diminished presence of monocytes and regulatory T cells (Tregs) subsets within the TME of HCC patients is correlated with a worsened prognosis

Given the variation in the abundance of immune cell infiltration in patients with HCC, we conducted an analysis to examine the relationship between tumor-infiltrating immune cells and prognosis. Our findings, illustrated in Fig. 10, indicate that decreased levels of monocytes and regulatory T cells (Tregs) infiltration were correlated with a reduced survival rate among HCC patients.

#### Discussion

Numerous studies have demonstrated the correlations between specific TMEM family proteins and tumor advancement<sup>16</sup>. However, to date, there is a lack of research on the expression of TMEM101 and its potential prognostic significance in HCC. Therefore, this study aims to investigate the potential role of TMEM101 in HCC.

Zhang *et al.*<sup>17</sup> demonstrated a significant upregulation of TMEM43 in HCC and noted that its inhibition led to a marked suppression of tumor development. Duan *et al.*<sup>9</sup> similarly observed an overexpression of TMEM106C in HCC, with its absence in SMMC-7721 cells resulting in inhibited proliferation and metastasis through the targeting of CENPM and DLC-1. Furthermore, the upregulation of TMEM106C was found to be

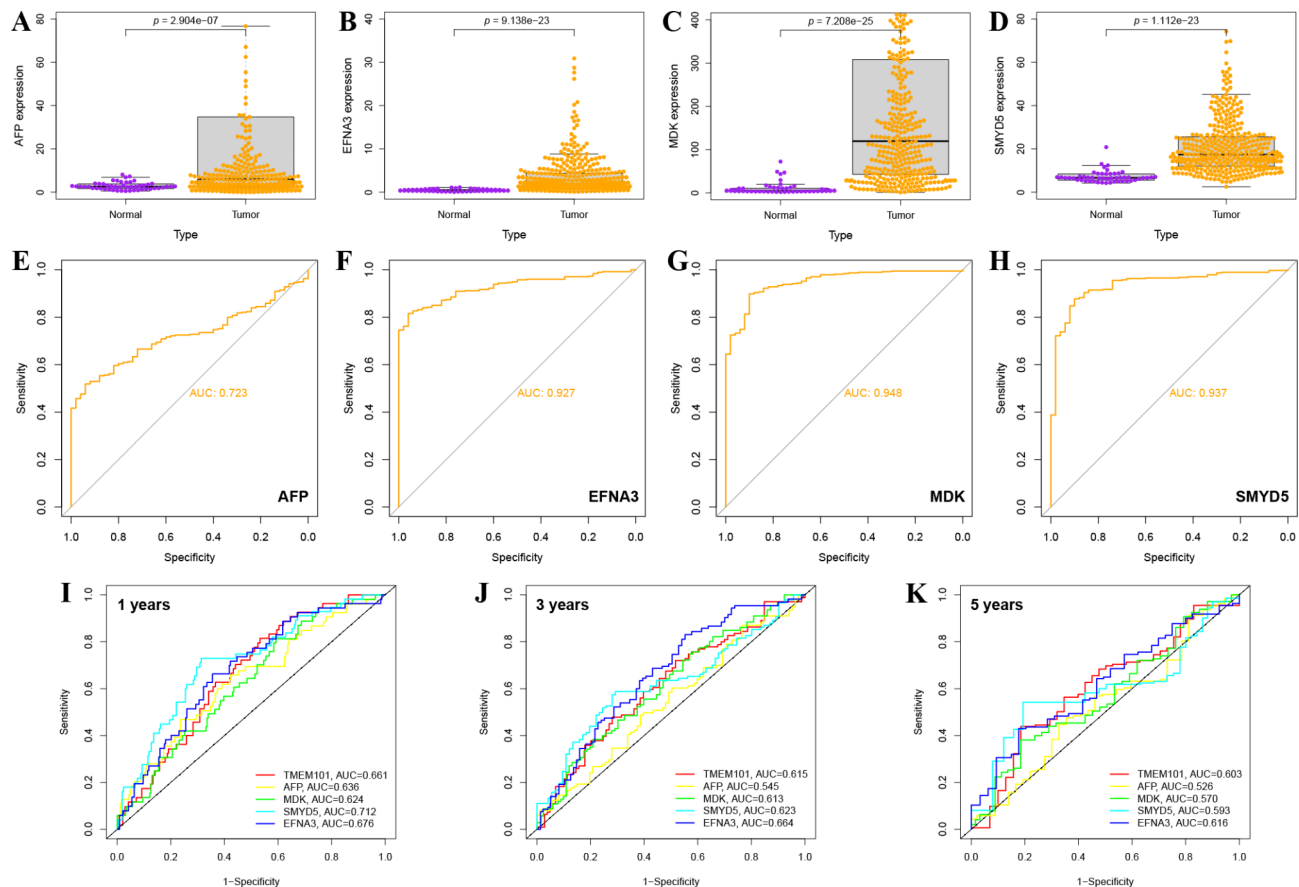


**Fig. 7.** TMEM101 was compared with other published biomarkers for its diagnostic effectiveness. **(A–D)** The expression levels of AFP **(A)**, EFNA3 **(B)**, MDK **(C)**, and SMYD5 **(D)** in HCC and normal liver tissues. **(E–H)** The ROC curve demonstrated the diagnostic value of AFP **(E)**, EFNA3 **(F)**, MDK **(G)**, and SMYD5 **(H)** in HCC patients. **(I–K)** The time-dependent ROC curves of the AFP, EFNA3, MDK, and SMYD5 were compared for 1-, 3-, and 5-year OS in HCC, respectively.

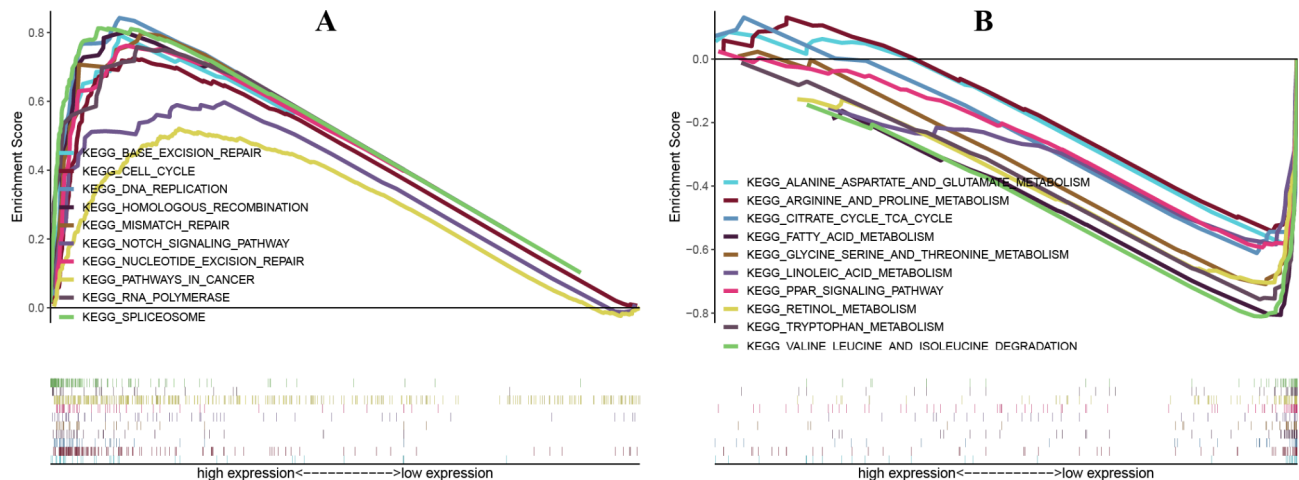


**Fig. 8.** Enrichment plots from gene set enrichment analysis (GSEA). **(A–B)** Multiple-GSEA results show KEGG<sup>35–37</sup> pathways are differentially enriched in high **(A)** and low **(B)** TMEM101 expression phenotypes. For previous uses, the Kanehisa laboratory have happily provided permission. The cutoff criterion was set at  $p < 0.05$ , and FDR  $< 0.05$  was considered statistically significant.

MSigDB collection	Gene set name	NES	NOM p-val	FDR q-val
c5.all.v2023.2.Hs.symbols.gmt	KEGG_SPLICEOSOME	2.15	0.000	0.000
	KEGG_DNA_REPLICATION	2.05	0.000	0.000
	KEGG_BASE_EXCISION_REPAIR	1.95	0.000	0.000
	KEGG_CELL_CYCLE	1.91	0.000	0.000
	KEGG_HOMOLOGOUS_RECOMBINATION	1.91	0.000	0.000
	KEGG_NUCLEOTIDE_EXCISION_REPAIR	1.91	0.000	0.000
	KEGG_MISMATCH_REPAIR	1.85	0.000	0.000
	KEGG_RNA_POLYMERASE	1.81	0.000	0.000
	KEGG_NOTCH_SIGNALING_PATHWAY	1.49	0.003	0.018
	KEGG_PATHWAYS_IN_CANCER	1.42	0.000	0.031

**Table 3.** Gene sets enriched in phenotype high. NES: normalized enrichment score; NOM: nominal; FDR: false discovery rate. Gene sets with NOM *p*-val < 0.05 and FDR *q*-val < 0.05 are considered as significant.

MSigDB collection	Gene set name	NES	NOM p-val	FDR q-val
c5.all.v2023.2.Hs.symbols.gmt	KEGG_FATTY_ACID_METABOLISM	-3.87	0.000	0.000
	KEGG_VALINE_LEUCINE_AND_ISOLEUCINE_DEGRADATION	-3.42	0.000	0.000
	KEGG_RETINOL_METABOLISM	-3.23	0.000	0.000
	KEGG_TRYPTOPHAN_METABOLISM	-3.21	0.000	0.000
	KEGGARGININE_AND_PROLINE_METABOLISM	-3.01	0.000	0.000
	KEGG_GLYCINE_SERINE_AND_THREONINE_METABOLISM	-2.86	0.000	0.000
	KEGG_LINOLEIC_ACID_METABOLISM	-2.50	0.000	0.000
	KEGG_PPAR_SIGNALING_PATHWAY	-2.47	0.000	0.000
	KEGG_CITRATE_CYCLE_TCA_CYCLE	-2.47	0.000	0.000
	KEGG_ALANINE ASPARTATE_AND GLUTAMATE_METABOLISM	-2.31	0.000	0.000

**Table 4.** Gene sets enriched in phenotype low. NES: normalized enrichment score; NOM: nominal; FDR: false discovery rate. Gene sets with NOM *p*-val < 0.05 and FDR *q*-val < 0.05 are considered as significant.

significantly associated with sex, tumor stage, grade, and prognosis in HCC patients<sup>9</sup>. Chen *et al.*<sup>18</sup> observed an upregulation of TMEM201 mRNA and protein levels in HCC, with high TMEM201 expression being linked to a poorer OS in HCC patients. Additionally, decreased TMEM201 expression was found to reduce the proliferation and migratory capabilities of HCC cells<sup>18</sup>. In contrast, Rao *et al.*<sup>16</sup> demonstrated that low TMEM205 expression was independently associated with a worse OS in HCC patients. Consequently, we aimed to analyze TCGA data to investigate the expression levels of TMEM101 and its relationship with clinicopathological features and prognosis in HCC. Our findings demonstrate a correlation between elevated TMEM101 expression and poor prognosis in HCC, similar to the relationship observed with TMEM106C<sup>9</sup>.

In this study, *in situ* hybridization staining revealed that TMEM101 mRNA is significantly overexpressed in liver cancer tissues compared to adjacent normal tissues. Moreover, high levels of TMEM101 expression in HCC were significantly linked to advanced tumor grade and stage. Cox regression analysis revealed an independent association between TMEM101 expression and HCC patient prognosis. Additionally, the ROC curve and calibration curves indicated that TMEM101, along with a nomogram combining TMEM101 and tumor stage, exhibited strong diagnostic value for HCC. These results suggest that TMEM101 may serve as a novel oncogene and a potential biomarker for independent prognostic assessment in HCC.

HCC is a prominent contributor to cancer-related mortality on a global scale. The management of HCC poses significant challenges, with early detection playing a crucial role in treatment efficacy<sup>19</sup>. The integration of liver ultrasound and AFP testing has emerged as a fundamental strategy for the surveillance of early-stage HCC. When utilized in combination, these diagnostic tools have demonstrated a pooled sensitivity increase from 45 to 63%. Conversely, AFP testing in isolation exhibits inadequate sensitivity levels and is typically not endorsed for HCC surveillance purposes<sup>20</sup>. It is imperative to explore new biomarkers in order to enhance the precision of early-stage HCC detection.

This study compared the diagnostic efficacy of TMEM101 with four established diagnostic biomarkers (AFP, EFNA3, MDK, and SMYD5) for HCC. AFP is a tumor-associated antigen that is typically silenced in normal adult hepatocytes but reactivated in HCC, impacting the viability and function of human natural killer (NK) cells, dendritic cells, and monocytes<sup>21,22</sup>. Ephrin-A3 (EFNA3) is a member of the Ephrin family of membrane-bound ligands, which are associated with the largest receptor tyrosine kinase (RTK) family known as Eph receptors. Husain *et al.*<sup>23</sup> demonstrated an upregulation of EFNA3 expression in HCC which was associated with decreased survival rates. Subsequent investigations revealed that the Ephrin-A3/EphA2 axis plays a role in modulating cellular metabolic plasticity to promote cancer stemness in hypoxic HCC<sup>23</sup>. Recently, SMYD5 has been recognized as a histone methyltransferase<sup>24</sup>. Chi *et al.*<sup>15</sup> observed that elevated levels of SMYD5 expression

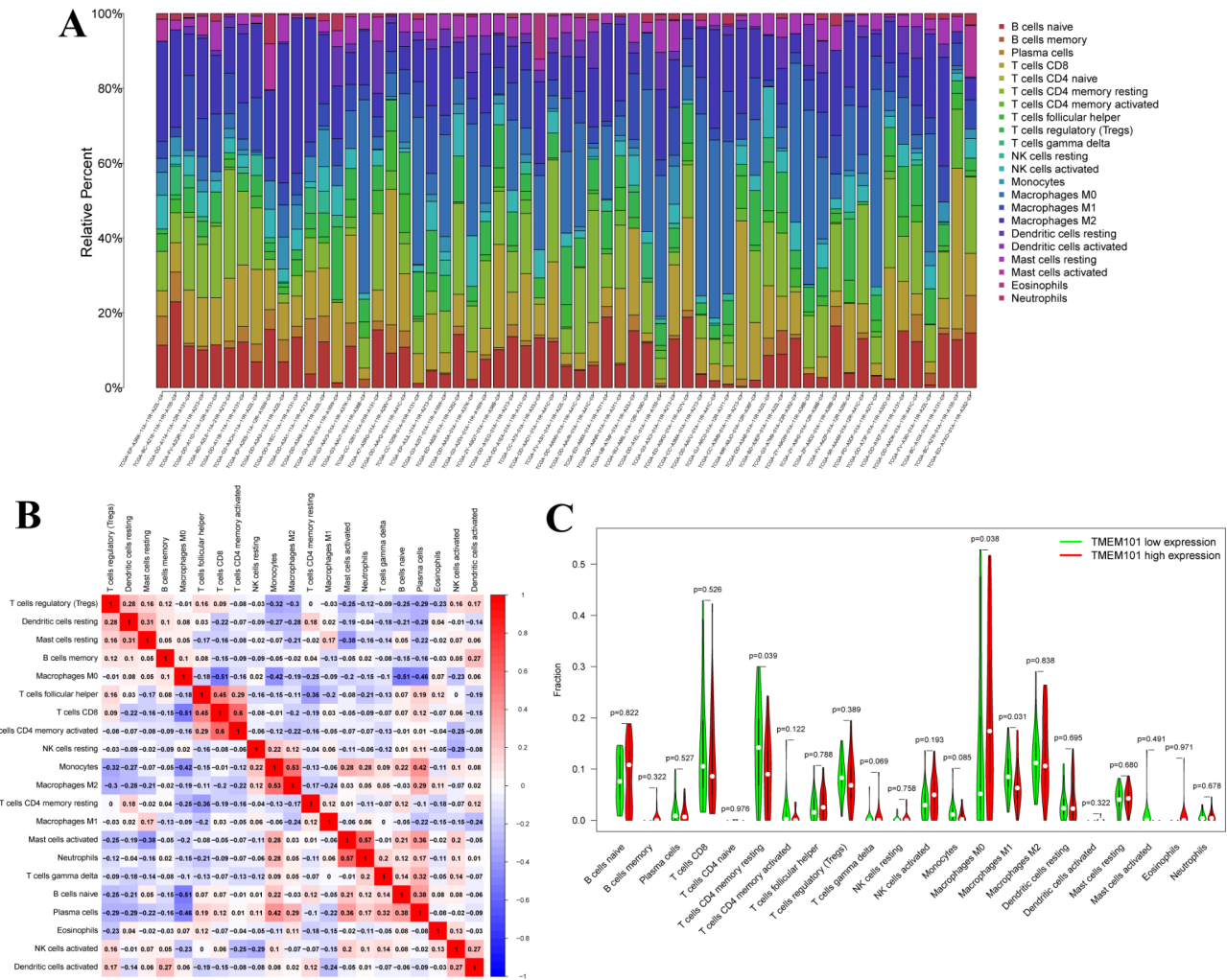


**Fig. 9.** Immune cells in HCC. (A) Estimated 22 immune leucocyte fractions in HCC by CIBERSORT algorithm. Each chart exhibited the cell proportions of each patient, and 22 immune leucocytes were in different colors on the right. (B) Correlations between different immune cell proportions are shown. Red denotes a positive correlation, while blue denotes a negative correlation. (C) Immune cell fractions in the TMEM101 low expression group (green) and the TMEM101 high expression group (red).

were associated with an unfavorable prognosis in HCC. The pro-angiogenic factor midkine (MDK) is a versatile secreted protein with cytokine and growth factor properties, modulating various signaling pathways and playing a role in essential cellular processes including proliferation, migration, and survival<sup>14</sup>. Numerous studies have demonstrated that MDK serves as a robust biomarker for the early detection of HCC<sup>25–27</sup>. The findings of our study indicate that the AUC values of the five diagnostic genes analyzed through ROC curve analysis were ranked as follows: TMEM101 > MDK > SMYD5 > EFNA3 > AFP. Time-dependent ROC curves revealed that the diagnostic efficacy of the five genes followed the order of EFNA3 > TMEM101 > SMYD5 > MDK > AFP. These results provide additional evidence supporting the potential of TMEM101 as a diagnostic and prognostic biomarker for HCC.

Chen *et al.*<sup>18</sup> screened four aberrant TMEM expression genes (TMEM106C, TMEM201, TMEM164, and TMEM45A) in HCC and subsequently developed a TMEMs signature based on their findings. Additionally, the results of GO and KEGG analyses suggest that the TMEMs signature may have significant implications in cell-cycle-related and immune-related pathways. Therefore, leveraging the TCGA data, we further investigated the signal transduction pathway of TMEM101 through GSEA. Furthermore, the relationship between TMEM101 and infiltrating immune cells was examined using CIBERSORT analysis. Similarly, analysis of KEGG pathways indicated that the high TMEM101 expression phenotype is significantly enriched in pathways related to cell cycle, DNA replication, and repair. Conversely, pathways involving amino acids, retinol, fatty acids, and linoleic acid metabolism are differentially enriched in the low TMEM101 expression phenotype. Overall, these findings suggest that TMEM101 may have a substantial impact on the regulation of HCC proliferation.

HCC is a type of cancer that is closely linked to inflammation, with over 90% of HCC cases attributed to hepatic injury and chronic inflammation. Prolonged and unresolved inflammation can result in the infiltration of immune cells into the liver, promoting tissue remodeling and potentially initiating and advancing the development

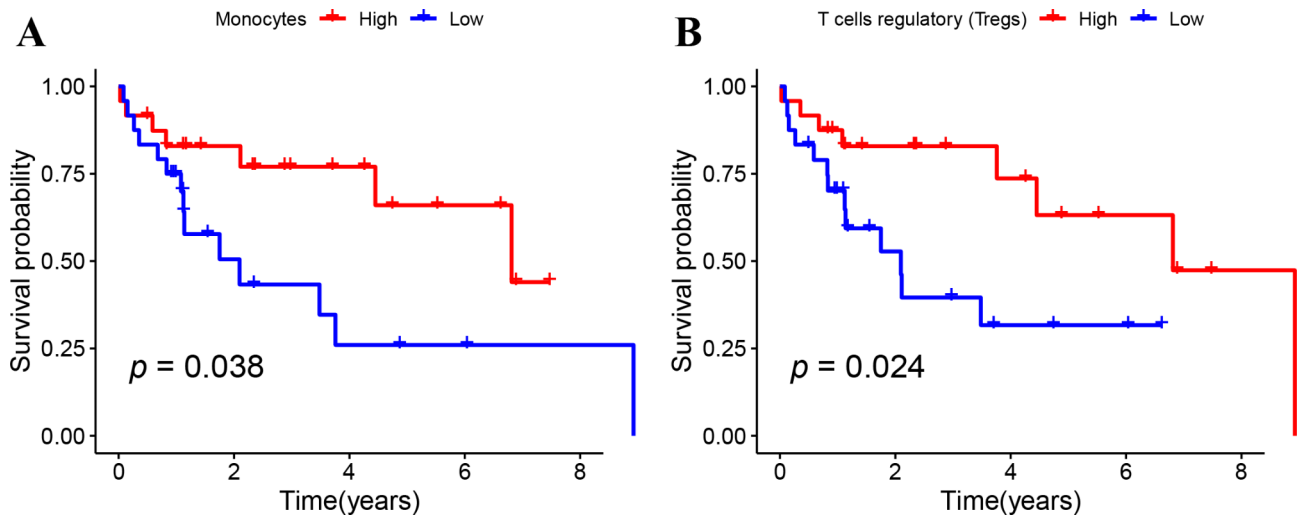


**Fig. 10.** Effect of tumor-infiltrating immune cell levels on the survival of HCC patients. **(A–B)** Kaplan-Meier analysis showed that lower infiltration levels of monocytes **(A)** and regulatory T cells (Tregs) **(B)** were associated with a poor prognosis in HCC patients.

of HCC<sup>28</sup>. For instance, Chen *et al.*<sup>29</sup> observed a high expression of resting memory CD4<sup>+</sup> T cells in HCC, which was identified as a protective factor for OS. Zhang *et al.*<sup>30,31</sup> noted that higher fractions of M0 macrophages were associated with a poorer prognosis in HCC. It is widely recognized that tumor-associated macrophages (TAMs) can exist in two distinct states: anti-tumor M1 macrophages and pro-tumor M2 macrophages<sup>32</sup>. Notably, our analysis in Fig. 9C reveals that compared to the group with low TMEM101 expression, the TMEM101 high expression group exhibited significantly decreased levels of infiltrating resting memory CD4<sup>+</sup> T cells and M1 macrophages, alongside a notable increase in M0 macrophage infiltration. Furthermore, our findings suggest a correlation between high TMEM101 expression and unfavorable prognosis in HCC. Hence, the findings suggest that TMEM101 may play a role in facilitating the initiation and progression of HCC through its impact on the infiltration of distinct immune cell populations. Additional research is necessary to corroborate these results.

## Conclusion

In conclusion, our study establishes TMEM101 expression as a novel independent prognostic factor in patients with HCC. Furthermore, we observed that elevated TMEM101 expression in HCC may be attributed to decreased promoter methylation levels compared to normal control samples. Specifically, our findings indicate that the oncogenic impact of heightened TMEM101 expression could be attributed to the suppression of anti-tumor cells (M1 macrophages and resting memory CD4<sup>+</sup> T cells) and promotion of M0 macrophage infiltration within the TME. These results revealed that high TMEM101 expression correlates with poor prognosis in HCC.

## Materials and methods

### Data mining in the TCGA database

Gene expression profile data of HCC patients were obtained from the Cancer Genome Atlas (TCGA) database (<https://portal.gdc.cancer.gov/>), encompassing 50 normal liver tissues and 374 HCC tissue samples. Clinical characteristics of 377 HCC patients were also retrieved from the TCGA. Subsequently, R software (version 4.2.3) was utilized for comprehensive analysis of RNA-Seq gene expression HTSeq-Counts data and clinical information of HCC patients. The expression levels of TMEM101 in normal liver and HCC tissues were visualized using Boxplots and a paired differential plot.

### Cell culture

The human hepatocytes L-02 and HCC cell lines SMMC7721, HepG2, HCCLM3 and MHCC97H were purchased from the Cell Resource Center at the Shanghai Institutes for Biological Sciences, Chinese Academy of Sciences (Shanghai, China). All cell lines were cultured in high-glucose DMEM supplemented with 10% FBS and 1% penicillin/streptomycin and incubated at 37°C in an atmosphere with 5% CO<sub>2</sub>.

### Quantitative real-time polymerase chain reaction (RT-qPCR)

Total RNA was extracted from normal hepatocytes and HCC cell lines using TRIzol reagent (Thermo Fisher Scientific, Waltham, MA, United States). Subsequently, 1 µg of total RNA from each sample was subjected to reverse transcription using the HiScript II Q RT superMix with gDNA Eraser (Vazyme, Nanjing, China) as a template for quantitative PCR (qPCR). The qPCR analysis was conducted on the CFX Connect real-time system (Bio-Rad, Hercules, CA, USA) with ChamQ Universal SYBR qPCR Master Mix (Vazyme) following the manufacturer's instructions. The thermal cycling procedure consisted of an initial denaturation step at 95°C for 30 s, followed by 40 cycles of denaturation at 95°C for 10 s and extension at 60°C for 30 s. The relative expression

levels of TMEM101 were normalized to  $\beta$ -actin and analyzed using the  $2^{-\Delta\Delta CT}$  method. The primers utilized for qPCR in this investigation were synthesized by BGI Corporation (Shenzhen, P.R. China). The primer sequences were displayed in Supplementary Table S1.

### Western blot analysis

Western blot analysis was conducted in accordance with established protocols that have been previously described<sup>33</sup>. Briefly, each sample containing 40  $\mu$ g of total protein was separated using an ExpressPlus PAGE Gel (4–20%, 15 wells) from Genscript and transferred to a 0.22  $\mu$ m PVDF membrane (Bio-Rad) via a semidry transfer system (Bio-Rad). The TMEM101 polyclonal antibody (Thermo Fisher, #PA5-102016) was diluted 1:5000, and the  $\beta$ -actin mouse monoclonal antibody (Beyotime, #AF0003) was diluted 1:8000.

### Tissue microarrays (TMA) and *in situ* hybridization.

Seventy-one formalin-fixed, paraffin-embedded tissue sections were used to create HCC tissue microarrays as per Nocito *et al.*'s method<sup>34</sup>. Tissue sections and clinical data (Supplementary Table S4) from HCC patients at Jiangxi Provincial People's Hospital were collected between March 2022 and December 2023. Inclusion criteria were a confirmed HCC diagnosis, no prior chemotherapy or radiation, comprehensive hospitalization records, and over 5 years of residency in Nanchang. Exclusion criteria were metabolic and infectious diseases, history of other tumors, previous radiotherapy or chemotherapy, and incomplete clinical data.

The *in situ* hybridization experiment involved washing the tissue microarrays with a series of solvents (xylene I and II, anhydrous ethanol I and II, 85% alcohol, 75% alcohol, and DEPC water). The arrays were then boiled in a repair solution for 10 min and allowed to cool. Protease K (20  $\mu$ g/ml) was added for digestion at 37 °C for 20 min. After rinsing with pure water and PBS (3 times for 5 min each), 3% methanol- $H_2O_2$  was added and incubated in the dark at room temperature for 15 min. The slides were washed three times in PBS (pH 7.4) for 5 min each to block endogenous peroxidase. They were then incubated with pre-hybridization solution at 37 °C for 1 h. After removing the pre-hybridization solution, a hybrid solution containing a mixed probe targeting different regions of the TMEM101 gene (Supplementary Table S2), designed and synthesized by Wuhan Servicebio Technology (Wuhan, China), was added. Wash the hybrid solution with 2  $\times$  SSC at 37 °C for 10 min, then with 1  $\times$  SSC at 37 °C for 2  $\times$  5 min, and finally with 0.5  $\times$  SSC at room temperature for 10 min. For more non-specific hybrids, increase formamide washing. Add normal rabbit serum and incubate at room temperature for 30 min. Then, add mouse anti-digoxin labeled peroxidase (anti-DIG-HRP), incubate at 37 °C for 40 min, and wash with PBS 4 times for 5 min each. Once the slides are slightly dried, add freshly prepared DAB solution and monitor the color development under a microscope until a brown-yellow color appears. Stop the reaction by rinsing with pure water. Restain with Harris hematoxylin for about 3 min, wash with tap water, revert to blue with ammonia, and rinse with running water. Immerse the slides sequentially in 75% alcohol for 6 min, 85% alcohol for 6 min, 100% alcohol I for 6 min, 100% alcohol II for 6 min, n-butanol for 6 min, and xylene for transparency. Remove the slides from xylene, let them dry slightly, and seal with neutral gum. Finally, perform microscopic examination, image acquisition, and analysis.

### Assessment of *in situ* hybridization staining

Servicebio's Aipathwell software was utilized to identify tissue regions and compute the H-Score in *in situ* hybridization staining. The H-Score method quantifies tissue staining by converting the intensity of positively stained cells into numerical values for semi-quantitative analysis.  $H\text{-Score} = \sum (p_i \times i) = (percentage\ of\ weak\ intensity\ cells \times 1) + (percentage\ of\ moderate\ intensity\ cells \times 2) + (percentage\ of\ strong\ intensity\ cells \times 3)$ . In the formula, "i" denotes cell positivity levels: 0 for negative, 1 for weakly positive, 2 for moderately positive, and 3 for strongly positive. "pi" indicates the proportion of positive cells. The H-score, ranging from 0 to 300, measures positivity intensity. The positive rate is the ratio of positive cells to the total cell count.

### Mutation and promoter methylation level

The study assessed the genetic alterations in TMEM101 and their correlation with OS and disease-free survival (DFS) in patients with HCC through analysis of the cBioPortal database (<https://www.cbioportal.org/>). Additionally, the promoter methylation status of TMEM101 in HCC and its subgroups was examined utilizing the UALCAN database (<https://ualcan.path.uab.edu/analysis.html>). The Student's *t*-test produced *p*-values, and even after Bonferroni correction for multiple measures, the *p*-value remained  $< 0.05$ , indicating statistical significance.

### Gene set enrichment analysis (GSEA)

GSEA was conducted to identify genes that exhibit correlation with TMEM101 gene expression in recent research studies and to investigate the notable survival disparities between high- and low-TMEM101 groups. In each analysis, gene set permutation was iterated 1000 times.

### Tumor-infiltrating immune cell profile

The tumor-infiltrating immune cells (TICs) abundance distributions of HCC patients were assessed using the CIBERSORT computational method. Subsequently, the relative proportions of 22 distinct immune cell types were compared between groups with high and low expression of TMEM101, and the findings were visually represented in a landscape map. Following this, prognostic analysis was conducted by calculating the abundance of 22 key immune cell types from a sample size of 424, based on survival data. The prognostic value of these immune cells was evaluated using univariate Cox regression analysis.

## Statistical analysis

Statistical analysis was conducted using R software version 4.2.3, employing the Kruskal-Wallis test for multiple continuous independent samples, the Wilcoxon signed-rank test for two continuous independent samples, and logistic regression to examine the association between TMEM101 and clinical characteristics in patients with HCC. Patients with incomplete clinical data were excluded from the analysis. Univariate and multivariate Cox regression analyses were subsequently performed to assess the impact of TMEM101 and clinical variables on OS, with the cutoff value for TMEM101 expression determined based on median values. The bar graph of RT-qPCR results in this study was performed using GraphPad Prism 5 software. A *p*-value < 0.05 was considered statistically significant.

## Data availability

The data presented in this study are openly available in the TCGA database [<https://portal.gdc.cancer.gov/>, (accessed on 22 April 2019)] and GEO database [<https://www.ncbi.nlm.nih.gov/geo/>, (accessed on 26 May 2017)].

Received: 9 July 2024; Accepted: 12 December 2024

Published online: 30 December 2024

## References

- Wang, W., Zhou, Y., Li, W., Quan, C. & Li, Y. Claudins and hepatocellular carcinoma. *Biomed. Pharmacother.* **171**, 116109 (2024).
- Luo, X. et al. Hepatocellular carcinoma: Signaling pathways, targeted therapy, and immunotherapy. *MedComm* **2024**(5), e474 (2020).
- Ntellas, P. & Chau, I. Updates on systemic therapy for hepatocellular carcinoma. *Am. Soc. Clin. Oncol. Educ. Book.* **44**, e430028 (2024).
- Christou, C., Stylianou, A. & Gkretsi, V. Midkine (MDK) in Hepatocellular Carcinoma: More than a Biomarker. *Cells* **13** (2024).
- Llovet, J. M. et al. Immunotherapies for hepatocellular carcinoma. *Nat. Rev. Clin. Oncol.* **19**, 151–172 (2022).
- Li, X. Y., Shen, Y., Zhang, L., Guo, X. & Wu, J. Understanding initiation and progression of hepatocellular carcinoma through single cell sequencing. *Biochim. Biophys. Acta Rev. Cancer* **1877**, 188720 (2022).
- Wang, Z., Wang, Y., Gao, P. & Ding, J. Immune checkpoint inhibitor resistance in hepatocellular carcinoma. *Cancer Lett.* **555**, 216038 (2023).
- Finn, R. S. et al. Atezolizumab plus Bevacizumab in unresectable hepatocellular carcinoma. *N Engl. J. Med.* **382**, 1894–1905 (2020).
- Duan, J. et al. TMEM106C contributes to the malignant characteristics and poor prognosis of hepatocellular carcinoma. *Aging (Albany NY)* **13**, 5585–5606 (2021).
- Schmit, K. & Michiels, C. TMEM proteins in cancer: A review. *Front. Pharmacol.* **9**, 1345 (2018).
- Matsuda, A. et al. Large-scale identification and characterization of human genes that activate NF- $\kappa$ B and MAPK signaling pathways. *Oncogene* **22**, 3307–3318 (2003).
- Gao, Q. et al. Integrated proteogenomic characterization of HBV-related hepatocellular carcinoma. *Cell* **179** 561–7. (2019).
- Chen, W. et al. Aberrant AFP expression characterizes a subset of hepatocellular carcinoma with distinct gene expression patterns and inferior prognosis. *J. Cancer.* **11**, 403–413 (2020).
- Lin, P. & Yang, H. EFNA3 is a prognostic biomarker for the overall survival of patients with hepatocellular carcinoma. *J. Hepatol.* **77**, 879–880 (2022).
- Chi, G. et al. SMYD5 acts as a potential biomarker for hepatocellular carcinoma. *Exp. Cell. Res.* **414**, 113076 (2022).
- Rao, J., Wu, X., Zhou, X., Deng, R. & Ma, Y. TMEM205 is an independent prognostic factor and is associated with immune cell infiltrates in hepatocellular carcinoma. *Front. Genet.* **11**, 575776 (2020).
- Zhang, N. et al. TMEM43 promotes the development of hepatocellular carcinoma by activating VDAC1 through USP7 deubiquitination. *Transl Gastroenterol. Hepatol.* **9**, 9 (2024).
- Chen, D. et al. Characterization of the clinical significance and immunological landscapes of a novel TMEMs signature in hepatocellular carcinoma and the contribution of TMEM201 to hepatocarcinogenesis. *Int. J. Mol. Sci.* **24** (2023).
- Johnson, P., Zhou, Q., Dao, D. Y. & Lo, Y. M. D. Circulating biomarkers in the diagnosis and management of hepatocellular carcinoma. *Nat. Rev. Gastroenterol. Hepatol.* **19**, 670–681 (2022).
- Tayob, N., Kanwal, F., Alsarraj, A., Hernaez, R. & El-Serag, H. B. The performance of AFP, AFP-3, DCP as biomarkers for detection of hepatocellular carcinoma (HCC): A Phase 3 biomarker study in the United States. *Clin. Gastroenterol. Hepatol.* **21**: (2023). 415–23.e4.
- Chen, X. et al. Prognostic biomarkers associated with immune checkpoint inhibitors in hepatocellular carcinoma. *Immunology* **172**, 21–45 (2024).
- Vujanovic, L. et al. Tumor-derived  $\alpha$ -fetoprotein directly drives human natural killer-cell activation and subsequent cell death. *Cancer Immunol. Res.* **5**, 493–502 (2017).
- Husain, A. et al. Ephrin-A3/EphA2 axis regulates cellular metabolic plasticity to enhance cancer stemness in hypoxic hepatocellular carcinoma. *J. Hepatol.* **77**, 383–396 (2022).
- Kidder, B. L., Hu, G., Cui, K. & Zhao, K. SMYD5 regulates H4K20me3-marked heterochromatin to safeguard ES cell self-renewal and prevent spurious differentiation. *Epigenetics Chromatin* **10**, 8 (2017).
- Zhu, W. W. et al. Evaluation of midkine as a diagnostic serum biomarker in hepatocellular carcinoma. *Clin. Cancer Res.* **19**, 3944–3954 (2013).
- Omran, M. M. et al. A combination of  $\alpha$ -fetoprotein, midkine, thioredoxin and a metabolite for predicting hepatocellular carcinoma. *Ann. Hepatol.* **19**, 179–185 (2020).
- Gowhari Shabgah, A. et al. Shedding more light on the role of Midkine in hepatocellular carcinoma: New perspectives on diagnosis and therapy. *IUBMB Life* **73**, 659–669 (2021).
- Sas, Z., Cendrowicz, E., Weinhäuser, I. & Rygiel, T. P. Tumor microenvironment of hepatocellular carcinoma: Challenges and opportunities for new treatment options. *Int. J. Mol. Sci.* **23** (2022).
- Chen, D., Li, X., Li, H., Wang, K. & Tian, X. Identification of immune-related prognostic mRNA and lncRNA in patients with hepatocellular carcinoma. *J. Oncol.* **2022** 5313149 (2022).
- Zhang, Z., Wang, Z. & Huang, Y. Comprehensive analyses of the infiltrating immune cell landscape and its clinical significance in hepatocellular carcinoma. *Int. J. Gen. Med.* **14**, 4695–4704 (2021).
- Zhang, Y., Zou, J. & Chen, R. An M0 macrophage-related prognostic model for hepatocellular carcinoma. *BMC Cancer* **22**, 791 (2022).
- Liu, Y. T., Mao, Z. W., Ding, Y. & Wang, W. L. Macrophages as targets in hepatocellular carcinoma therapy. *Mol. Cancer Ther.* **23**, 780–790 (2024).
- Pang, Y. et al. Inhibition of abnormally activated HIF-1 $\alpha$ -GLUT1/3-glycolysis pathway enhances the sensitivity of hepatocellular carcinoma to 5-caffeoquinic acid and its derivatives. *Eur. J. Pharmacol.* **920**, 174844 (2022).

34. Nocito, A. et al. Microarrays of bladder cancer tissue are highly representative of proliferation index and histological grade. *J. Pathol.* **194**, 349–357 (2001).
35. Kanehisa, M. & Goto, S. KEGG: kyoto encyclopedia of genes and genomes. *Nucleic Acids Res.* **28**, 27–30 (2000).
36. Kanehisa, M. Toward understanding the origin and evolution of cellular organisms. *Protein Sci.* **28**, 1947–1951 (2019).
37. Kanehisa, M., Furumichi, M., Sato, Y., Kawashima, M. & Ishiguro-Watanabe, M. KEGG for taxonomy-based analysis of pathways and genomes. *Nucleic Acids Res.* **51**, D587–d92 (2023).

## Author contributions

Conception and design: Q.G.F. and L.Y.K; acquisition and analysis of data: L.Y.K. Y.L.P. and Q.G.F; funding acquisition, investigation and writing the manuscript: L.Y.K; supervision and edit: Q.G.F. All authors contributed to the article and approved the submitted version.

## Funding

This study was funded by the Jiangxi Provincial Health Technology Project (202130039 and 202510154).

## Declarations

### Competing interests

The authors declare no competing interests.

### Ethics approval and consent to participate

The study adhered to the Declaration of Helsinki and received approval from the Ethics Committee of Jiangxi Provincial People's Hospital (Approval No: 20240609). All participants signed the informed consents.

### Additional information

**Supplementary Information** The online version contains supplementary material available at <https://doi.org/10.1038/s41598-024-83174-0>.

**Correspondence** and requests for materials should be addressed to Q.F.

**Reprints and permissions information** is available at [www.nature.com/reprints](http://www.nature.com/reprints).

**Publisher's note** Springer Nature remains neutral with regard to jurisdictional claims in published maps and institutional affiliations.

**Open Access** This article is licensed under a Creative Commons Attribution-NonCommercial-NoDerivatives 4.0 International License, which permits any non-commercial use, sharing, distribution and reproduction in any medium or format, as long as you give appropriate credit to the original author(s) and the source, provide a link to the Creative Commons licence, and indicate if you modified the licensed material. You do not have permission under this licence to share adapted material derived from this article or parts of it. The images or other third party material in this article are included in the article's Creative Commons licence, unless indicated otherwise in a credit line to the material. If material is not included in the article's Creative Commons licence and your intended use is not permitted by statutory regulation or exceeds the permitted use, you will need to obtain permission directly from the copyright holder. To view a copy of this licence, visit <http://creativecommons.org/licenses/by-nc-nd/4.0/>.

© The Author(s) 2024